Marine Chemistry 211 (2019) 15–24

Contents lists available at ScienceDirect

Marine Chemistry

journal homepage: www.elsevier.com/locate/marchem

# Exploring sediment porewater dissolved organic matter (DOM) in a mud volcano: Clues of a thermogenic DOM source from fluorescence spectroscopy

Simona Retelletti Brogi[a], Ji-Hoon Kim[b], Jong-Sik Ryu[c], Young Keun Jin[d], Yun Kyung Lee[a], Jin Hur[a,*]

[a] Department of Environment & Energy, Sejong University, Seoul 05006, South Korea
[b] Division of Petroleum and Marine Research, Korea Institute of Geoscience and Mineral Resources, Daejeon 34133, South Korea
[c] Department of Earth and Environmental Sciences, Pukyong National University, Busan 48513, South Korea
[d] Korea Polar Research Institute (KOPRI), Incheon 21990, South Korea

ARTICLE INFO

*Keywords:*
DOM
EEM-PARAFAC
Mud volcano
Deep fluid
Sediment

ABSTRACT

Mud volcanoes (MVs) are potential conduit migration pathways for deep thermogenic DOM. In this study, we investigated the dissolved organic matter (DOM) of porewater in a MV in the Canadian Beaufort Sea and compared dissolved organic carbon (DOC) and fluorescent DOM (FDOM) between the MV and a reference site (RS). The chemical and isotopic compositions ($Cl^-$, $\delta^{18}O$ and $\delta D$) of porewater from the MVs indicated that these fluids are derived from a mixture of seawater, meteoric water, and clay dehydration, causing a freshening of the porewaters. Interestingly, the porewaters in the MV exhibited DOC concentrations up to 14 times higher than those in the RS. This high DOC concentration was attributed to a higher concentration in the deep fluid moving upwards through the MV, and in minor part to processes such as particulate organic matter sulfate reduction, anaerobic oxidation of methane and higher biological activity in the MV sediments. The fluorescence results showed the presence of four components in both MV and RS sites, which included two humic-like, one microbial humic-like, and a protein-like component. All the four fluorescent components increased with depth, showing a good linear relationship with DOC. However, the DOC-normalized fluorescence in the porewater DOM was on average 3 to 7 times lower in the MV, suggesting that the DOM molecules have undergone thermogenic processes in the deep sediments, and that shallow processes do not affect significantly the FDOM composition. Our results highlight that fluids migrating from the deep sediment through the MV can be an important source of thermogenically altered DOM to the shallow sediments and overlaying water column.

## 1. Introduction

Dissolved organic matter (DOM) in marine sediments plays a key role in carbon and nitrogen remineralization as well as in carbon preservation in sediments (Burdige and Komada, 2015). Marine sediments are also considered to be an important source of DOM to the overlying seawaters. It has been estimated that DOC flux from coastal and continental margin sediments can reach ~350 Tg C $year^{-1}$ (Burdige and Komada, 2015), which is comparable to that estimated for rivers (Raymond and Spencer, 2015). The characteristics of the DOM released from sediments to the overlying water can affect the quantity and quality, and further the reactivity of DOM in the water column. The physical, chemical, and biological factors shaping the DOM properties in porewaters are affected by the conditions of the sediment itself (e.g., redox conditions, biological community, and sediment texture) (Burdige, 2007; Burdige and Komada, 2015; Chen and Hur, 2015; Dang et al., 2014; Henrichs, 1992; Komada et al., 2016; Qualls and Richardson, 2003; Schulz et al., 1994). Komada et al. (2013) suggested that sediment porewaters are indeed a mixture of compounds with different reactivity and isotopic signature. Therefore, porewater DOM is variable in time and space.

Mud volcanoes (MVs) are a unique environment found at seafloor, associated to the release of a large amount of methane and the presence of chemosynthetic biological communities (Lösekann et al., 2008). Their eruption is characterized by the so-called “mud breccia”, a mixture of hydrocarbon gas (mainly $CH_4$), carbon dioxide, nitrogen, helium, water, oil, mud and rock fragments (Cita et al., 1989; Kopf, 2002; Mazzini and Etiope, 2017). The morphology of the MV as well as the

* Corresponding author.
*E-mail address:* jinhur@sejong.ac.kr (J. Hur).

https://doi.org/10.1016/j.marchem.2019.03.009
Received 12 October 2018; Received in revised form 13 March 2019; Accepted 14 March 2019
Available online 16 March 2019
0304-4203/ 

sources of the fluids and sediments composing the mud breccia are highly variable and depend on the geological settings. The fluids' and sediments' ascent within the MVs has been attributed to their buoyancy. However, some recent studies proposed the porosity waves as a mechanism for the upward migration of deep fluids (Connolly and Podladchikov, 2016; Yarushina et al., 2015). A detailed review on mud volcanism was recently proposed by Mazzini and Etiope (2017).

The exact number of marine MVs is still unknown. However, Milkov (2000) estimated that approximately $10^3$ to $10^5$ deep water MVs exist worldwide, which are known to continuously expel fluids even during dormant periods (Dählmann and de Lange, 2003). The chemistry of the extruding fluids is the result of the fluid sources, sediment-water interactions occurring along the vertical conduits and to the characteristics of the environment, such as porosity, temperature and pressure gradients, the presence of gas hydrates, local tectonics, etc. (Mazzini and Etiope, 2017). Oxygen and hydrogen stable isotopes ($\delta^{18}O$ and $\delta D$) have been used as tracers in hydrological studies. Isotope fractionation will result from differences in the physical and chemical properties of the environment. Therefore, they can reflect the contribution of different sources and processes (Clark and Fritz, 1997; Gat, 1996; Kendall and Caldwell, 1998; Minami et al., 2018; West et al., 2014).

Many studies have been conducted on these environments to understand their geological settings and/or the chemistry of the extruded fluids (Dählmann and de Lange, 2003; Haese et al., 2006; Li et al., 2014; Loher et al., 2018; Pohlman et al., 2010). None of these studies, however, have paid any attention to the DOM in these unique environments. To the best of authors' knowledge, no study has been conducted to directly measure the DOM concentrations and/or properties in MV porewaters, although a few studies mentioned the importance of the DOM in similar environments. For example, Valentine et al. (2005) suggested that the DOC coming from a methane seep in the North Pacific might support the heterotrophic community, which in turn, facilitates the mobilization and degradation of autochthonous organic matter. Pohlman et al. (2010) have also suggested that sedimentary microbes could produce methane-derived DOC, in addition to carbon dioxide, from methane metabolism. Based on the estimates of the abundance of MVs (Milkov, 2000) using $\Delta^{14}C$ and $\delta^{13}C$ measurements, it was estimated that a potential flux of methane-derived DOC to the global deep ocean could be equivalent to $1.7 \times 10^{10}$ to $1.7 \times 10^{12}$ mol $yr^{-1}$. Meanwhile, Dittmar and Koch (2006) identified a major thermogenic DOM component in the deep Southern Ocean seawater using Fourier transform-ion cyclotron resonance technique (FT-ICR-MS), highlighting the importance of this DOM component in global biogeochemical cycles. These previous studies signified the need for quantification and characterization of DOM in mud volcanoes.

The optical properties of DOM have been extensively utilized in the last decade to characterize and identify the sources of organic matter in a wide range of environments. In particular, the fluorescence excitation-emission matrices (EEMs) coupled with parallel factor analysis (PARAFAC) allow the identification of the main groups of fluorophores and the capacity to distinguish between autochthonous and allochthonous sources of DOM (Chen et al., 2016; Osburn et al., 2016a; Walker et al., 2009; Wang et al., 2013; Yang et al., 2017).

This study aims to 1) characterize the DOM in the porewater of a MVs in the Canadian Beaufort Sea using the concentration (DOC) and its fluorescence properties and 2) delineate the DOM sources of porewater in the MVs based on the DOM quantity and the quality (fluorescence) as well as other chemical properties of the fluids (i.e., anions concentration, and oxygen and hydrogen isotopes). For this purpose, porewaters from four sites in a mud volcano (MV) region and one reference site (RS) in the Canadian Beaufort Sea were analyzed for the organic and inorganic properties.

Paull et al. (2015) confirmed the presence of this mud volcano at 420 m depth in the continental slope of the Canadian Beaufort Sea. The expulsion and consequent accumulation of the mud were attributed to overpressured biogenic methane. The chemical properties of the pore waters (between 0 and ~700 cm below the sea floor) in the MV (low chlorinity, high sodium, negative $\delta^{18}O$, and $\delta D$) were explained by a mixture of seawater, meteoric water and clay dehydration.

## 2. Methods

### 2.1. Study area

Three mud volcano structures were first revealed at ~282 m, ~420 m, and ~740 m depth by multibeam bathymetric mapping data collected on the continental slope of the Canadian Beaufort Sea in 2009 and 2010 (see http://www.omg.unb.ca/Projects/Arctic/google/for data catalog). Subsequent cruises were conducted in the fall of 2010 (2010-035-WD), 2012 (2012004PGC), 2013 (2013005PGC), and 2016 (2016006PGC) on the Canadian Coast Guard Icebreaker Sir Wilfred Laurier (SWL) and in the fall of 2013 (ARA04C), 2014 (ARA05C), and 2017(ARA08C) on the South Korean Icebreaker Araon to investigate the shelf edge and slope of the Canadian Beaufort Sea. Remotely operated vehicle (ROV) video observations and water column acoustic anomalies showed that these are young and actively forming features experiencing ongoing eruptions (Jin and Shipboard Scientific Party, 2018; Paull et al., 2015). The 420-m mud volcano is the biggest structure among the three volcanos. Its size is comparable with the Haakon Mosby Mud Volcano in the Barents Sea which is a typical example of an active marine mud volcano (Milkov et al., 2004). Details on the MV morphology and on the geological settings of this area can be found in (Paull et al., 2015). Briefly, the continental slope of the Canadian Beaufort Sea area is underlain by a thick sedimentary sequence of Mesozoic and Quaternary strata (Grantz and Hart, 2012). The Quaternary shelf sediments contain ice bonded permafrost down to 700 m and gas hydrates to 1200 m below sea floor (Paull et al., 2015 and references therein). Previous studies in the shelf edge and slope of the Beaufort Sea showed the occurrence of brackish porewaters associated with the decomposition of permafrost and regional hydraulic gradients (Frederick and Buffett, 2014; Paull et al., 2011, 2015; Taylor et al., 2013).

### 2.2. Sample collection

The samples were collected during the ARA08C cruise on September 2017 on board of the South Korean icebreaker, Araon. Sediment cores were taken using a box corer at four MV sites (Station 15, 16, 17, and 18) and one reference site (RS, Station 21). The RS is located > 1 km far from the border of the MV (Fig. 1, Table S1) and at the same depth (420 m). The influence of the emerging fluids from the MV is therefore negligible. Porewaters were slowly extracted from each core at approximately 8, 16, 24, 32 and 40 cm below seafloor (cmbsf) by using acid-washed Rhizon samplers (Rhizosphere Research Products). The extracted fluid samples were immediately filtered through a 0.2 µm, acid-washed polytetrafluoroethylene filter and stored in acid-washed polypropylene bottles at −20 °C until analysis. This preservation method was chosen due to the long time needed to receive the samples to the laboratory (~2 months) and we assume that it does not affect significantly the fluorescence properties of the DOM, as shown by Otero et al. (2007).

### 2.3. Analytical methods

After the porewater samples were melted at room temperature, dissolved organic carbon (DOC) was measured by a TOC analyzer (Shimadzu TOC-L) through high temperature catalytic oxidation.

Fluorescence excitation-emission matrices (EEMs) were measured with a Hitachi F-7000 fluorescence spectrophotometer. Excitation ranged 220 and 500 nm with a 5-nm interval, while emission encompassed between 280 and 550 nm with a 1-nm interval. The drEEM toolbox (Murphy et al., 2013) was used to perform EEMs correction

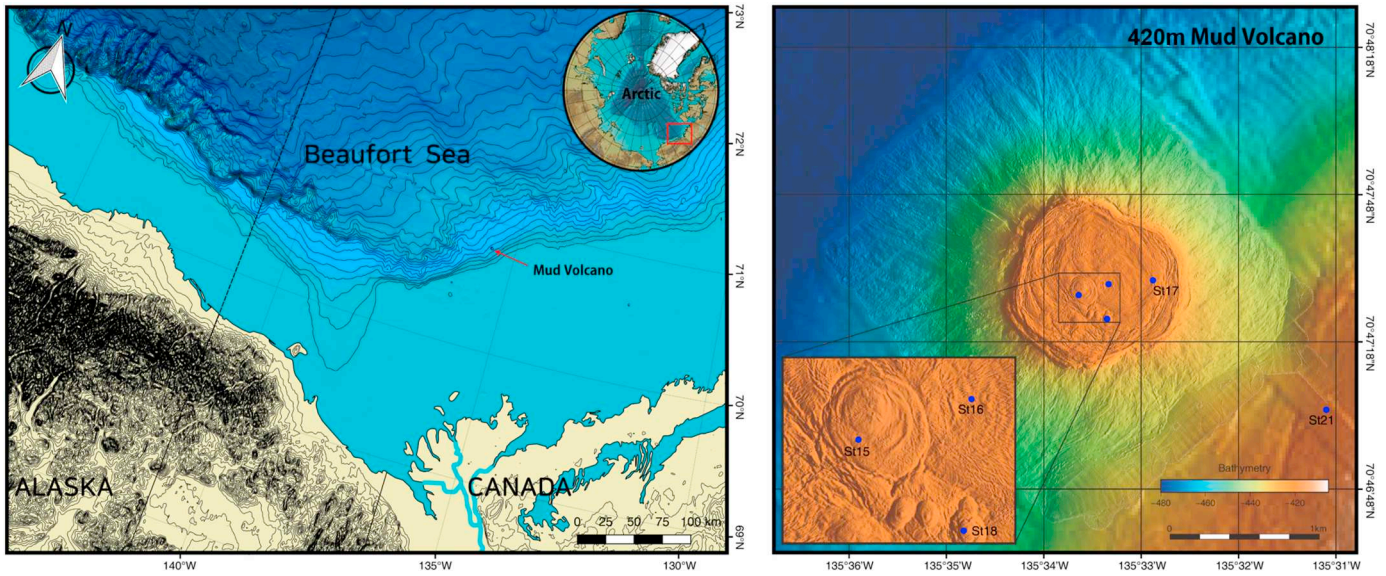


**Fig. 1.** Sampling area and sites. The bathymetry lines on the left figure are drawn every 100 m.

(e.g., blank subtraction, inner filter correction, and Raman normalization) and PARAFAC analysis. The inner filter correction was performed within the toolbox according to the following equation

$$F^{IFE} = I \bullet F$$

where I is a correction matrix calculated as follows

$$I_{\lambda_{ex}\lambda_{em}} = 10^{0.5(A_{\lambda ex} + A_{\lambda em})}$$

The absorbance ($A_\lambda$) was measured in a 1 cm quartz cuvette by using a Shimadzu UV-1800 UV spectrophotometer between 230 and 700 nm at 0.5 nm interval. More detail on the inner filter correction procedure within the toolbox can be found in Murphy et al. (2010).

The validation of the PARAFAC model was made by split half analysis and percentage of explained variance (99.63%). Specific fluorescence intensities of the PARAFAC components (C*) were calculated by dividing the fluorescence intensities of each sample by its DOC concentration. The C* provides the information on the changes in the composition of the fluorescent DOM (FDOM) pool as an intrinsic metric (Korak et al., 2014). By using corrected EEMs, the index of recent autochthonous DOM contribution, or biological index (BIX), was calculated as the ratio of the fluorescence intensity at the emission wavelength of 380 nm to 430 nm at an excitation wavelength of 310 nm (Huguet et al., 2009).

The following measurements on porewaters chemical composition were performed according to Gieskes et al. (1991) and Kim et al. (2013). The chloride ($Cl^-$) concentration and alkalinity were measured by titration with silver nitrate ($AgNO_3$) and with 0.02 N HCl, respectively. The reproducibility of $Cl^-$ and alkalinity was monitored by repeated analyses using the International Association of Physical Sciences of the Oceans (IAPSO) standard seawater and was < 2% and < 0.5%, respectively. $NH_4^+$ and $PO_4^{3-}$ were measured spectrophotometrically (Shimazu UV-2450) at 640 nm and 885 nm, respectively, at the Korea Institute of Geoscience and Mineral Resources (KIGAM). Sulfate ($SO_4^{2-}$) was analyzed by ion chromatography (ICS-1100, Dionex) at the Korea Basic Science Institute (KBSI). Total Fe and Mn were measured using an inductively coupled plasma atomic emission spectroscopy (ICP-AES; Optima 8300, Perkin Elmer, USA) at the KBSI. IAPSO standard seawater was also repeatedly analyzed to verify the analytical quality of the instruments and analytical reproducibility was better than ± 2% ($n$ = 3).

The isotopic composition (δD and $\delta^{18}O$) of the porewater was determined at the KIGAM with a wavelength-scanned cavity ring-down spectroscopy (L2120-i, Picarro) according to Jung et al. (2013). All δD and $\delta^{18}O$ values were denoted by delta (δ) notation relative to a standard (Vienna Standard Mean Ocean Water; VSMOW), where δ (‰) = $[(R_{sample}/R_{reference}) - 1] \times 1000$ and R represents $^2H/^1H$ and $^{18}O/^{16}O$. The analytical results were normalized with international standards: IAEA-VSMOW2, -SLAP and -GISP with assigned $\delta^{18}O$ and δD of 0‰ and 0‰, −55.50‰ and −427.5‰, and −24.76‰ and −189.5‰, respectively. Analytical reproducibility of $\delta^{18}O$ and δD were ± 0.1‰ and ± 0.5‰, respectively.

## 3. Results

To compare the characteristics of DOM and fluid chemistry in the porewaters of four MV versus RS sites, the average ( ± standard deviation) of each parameter for the four MV sites are taken into account. The data for each station are reported in Table S2.

### 3.1. PARAFAC results

PARAFAC analysis validated a four-component model (Fig. 2). Component 1 (C1) showed two excitation peaks with the primary one at < 250 nm and a secondary peak at 300 nm. The emission spectra exhibited a maximum at 425 nm. Component 2 (C2) showed both excitation and emission maxima at longer wavelengths with respect to C1. The excitation had a peak at < 250 nm and a broad shoulder with the maximum at 384 nm, while the emission presented a broad shoulder with the maximum at 526 nm. Component 3 (C3) had two excitation maxima at < 250 nm and 295 nm, and the emission maximum at 378 nm. Component 4 (C4) exhibited one excitation maximum at 270 nm and one emission peak at 309 nm.

### 3.2. Fluid composition and isotopic properties (MV versus RS sites)

The downcore profiles of porewater in the MV showed a decrease of chloride and sulfate, together with an increase of alkalinity, phosphate, and ammonium (Fig. 3, Table 1, Table S2). In the reference station (RS), on the contrary, these parameters showed a constant profile with depth (Fig. 3, Table 1, Table S2). Chloride concentration at the MV had the maximum value in the uppermost samples (8 cmbsf), ranging from 516 to 565 mM (average 540 ± 21 mM), which was similar to those of the Canadian Beaufort seawater (559 mM) (Paull et al., 2015), 2018) and the RS in this study (556 mM). The values exhibited a decreasing trend

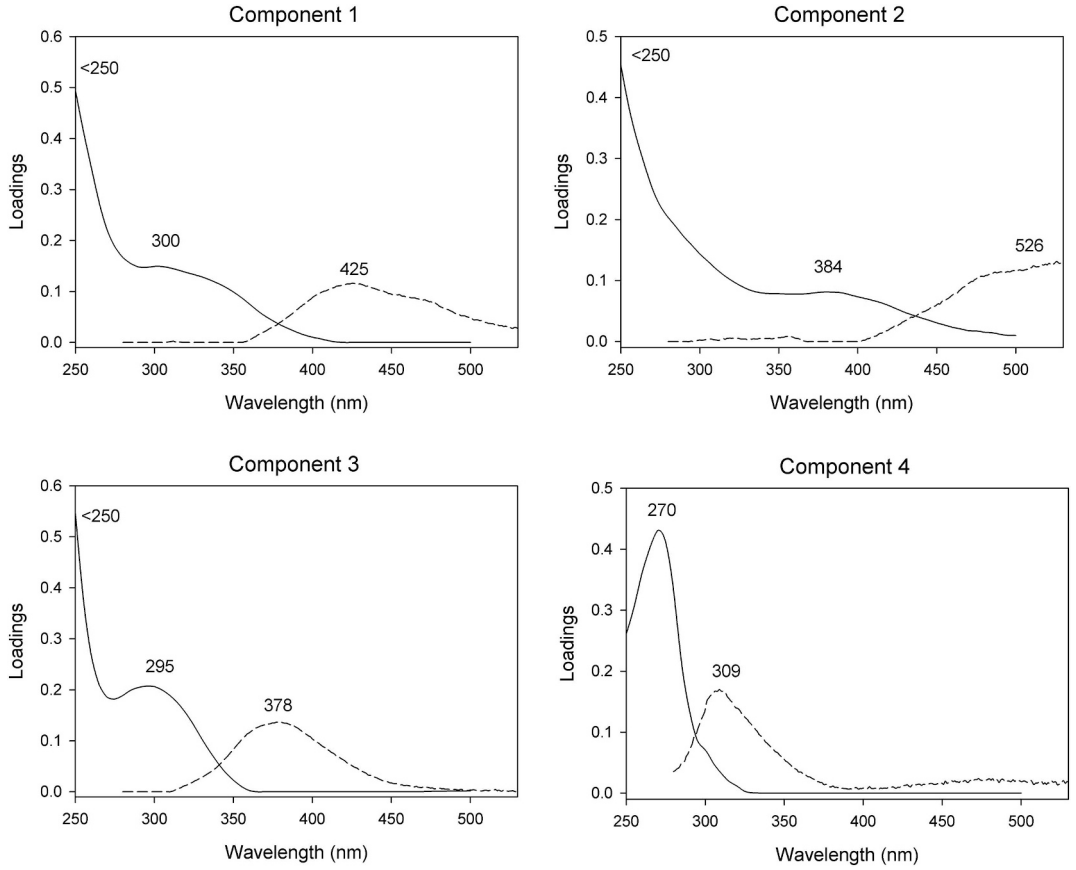


**Fig. 2.** Fluorescent components validated by PARAFAC analysis. The wavelengths of excitation (solid line) and emission (dotted line) maxima are highlighted on the figure.

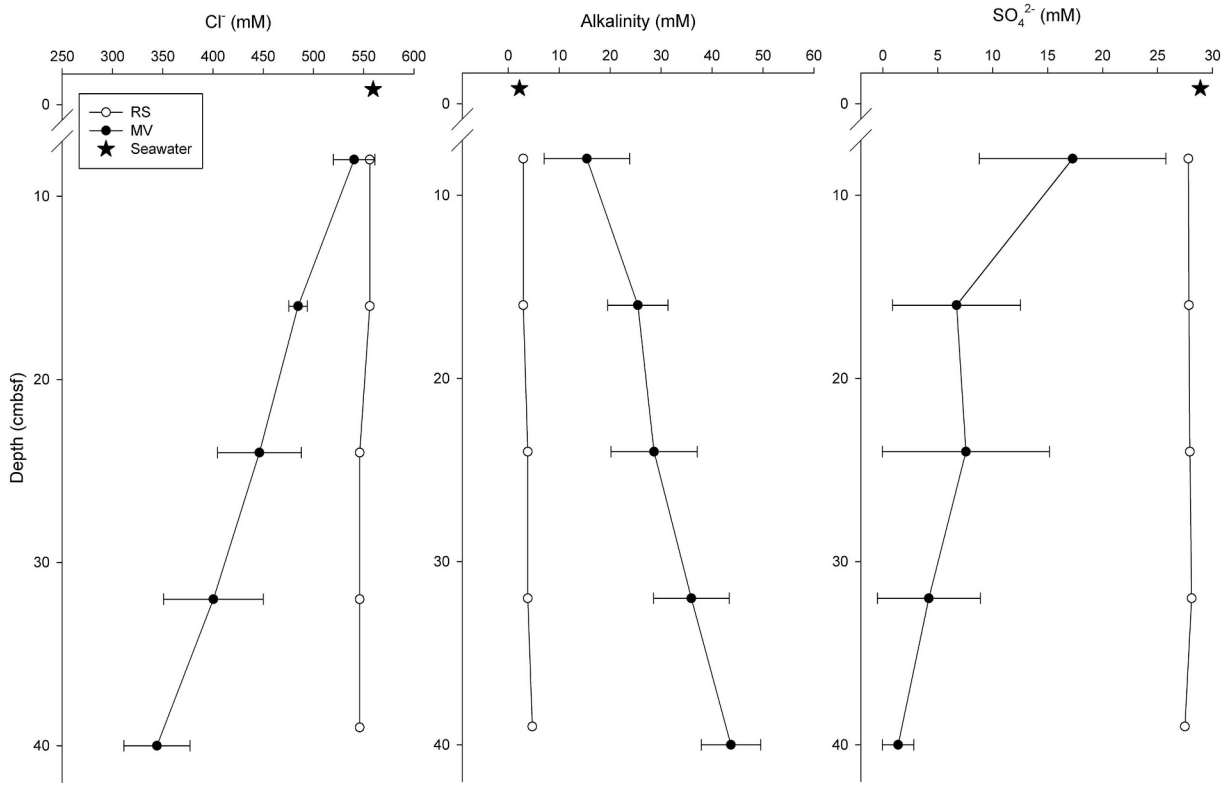


**Fig. 3.** Vertical profile of chloride, alkalinity, and sulfate in the mud volcano sites (MV, average ± standard deviation of the four stations), in the reference site (RS) and in seawater. The values in seawater in the same area are from Paull et al. (2015).

**Table 1**
Inorganic properties of porewaters in the mud volcano sites (average ± standard deviation of four stations) and a reference site.

| Station | Depth (cmbsf) | $Cl^-$ (mM) | Freshening (%) | Alkalinity (mM) | $SO_4^{2-}$ (mM) | $NH_4^+$ (mM) | $PO_4^{3-}$ (μM) | $\delta^{18}O$ (‰ VSMOW) | δD (‰ VSMOW) |
|---|---|---|---|---|---|---|---|---|---|
| Mud Volcano sites | 8 | 540.4 ± 20.7 | 3.5 ± 3.2 | 15.4 ± 8.4 | 17.3 ± 8.5 | 0.203 ± 0.210 | 30.6 ± 24.8 | −0.11 ± 0.18 | −1.79 ± 1.55 |
| | 16 | 484.6 ± 9.2 | 13.1 ± 1.6 | 25.4 ± 5.9 | 6.7 ± 5.8 | 0.406 ± 0.419 | 62.7 ± 22.8 | −0.43 ± 0.16 | −4.85 ± 1.99 |
| | 24 | 446.2 ± 41.7 | 20.0 ± 7.5 | 28.6 ± 8.5 | 7.6 ± 7.6 | 0.703 ± 0.559 | 92.5 ± 19.5 | −0.88 ± 0.22 | −9.39 ± 2.39 |
| | 32 | 400.4 ± 49.6 | 28.2 ± 8.9 | 35.9 ± 7.4 | 4.2 ± 4.7 | 1.009 ± 0.722 | 120.7 ± 39.7 | −1.49 ± 0.24 | −15.21 ± 2.48 |
| | 39 | 344.2 ± 32.9 | 38.3 ± 5.9 | 43.7 ± 5.8 | 1.4 ± 1.4 | 1.240 ± 0.492 | 137.1 ± 51.1 | −2.08 ± 0.19 | −21.55 ± 2.40 |
| Reference site | 8 | 556.1 | | 2.9 | 27.8 | 0.004 | n.d. | 0.31 | 1.47 |
| | 16 | 556.1 | | 2.9 | 27.9 | 0.029 | 8.8 | – | – |
| | 24 | 545.9 | | 3.8 | 27.9 | 0.069 | n.d. | 0.29 | 1.25 |
| | 32 | 545.9 | | 3.8 | 28.1 | 0.071 | n.d. | – | – |
| | 39 | 545.9 | | 4.7 | 27.5 | 0.240 | 1.9 | 0.27 | 1.69 |

–: not measured; n.d.: not detected.

with depth, ranging between 313 and 391 mM (average 344 ± 33 mM) at ~40 cmbsf in the MVs.

By using the measured chloride values in the MV site, a freshening ratio was calculated at each depth, expressed as a percentage of the seawater value, using the following equation (Kim et al., 2013):

$$Freshening = \frac{Cl^-_{sw} - Cl^-_{pw}}{Cl^-_{sw}} x\ 100$$

where $Cl^-_{pw}$ is the chloride concentration in the porewater of MV sites and $Cl^-_{sw}$ is the value in the Canadian Beaufort seawater (i.e., 559 mM).

The freshening ratio in the uppermost samples ranged between 0 and 7.6% (average 3.5 ± 3.2%) and sharply increased with depth, ranging between 30.0 and 43.8% (average 38.3 ± 5.9%) at 40 cmbsf (Table 1 and Table S2).

Alkalinity in the RS had the values similar to the Canadian Beaufort seawater (2.2 mM, Paull et al., 2015) at all the depths (average of 3.7 ± 0.7 mM). In contrast, it was ~5 times higher (15.4 ± 8.4 mM) in the uppermost samples and ~9 times higher at 40 cmbsf in the MV site compared to that in the RS (4.7 mM) (Fig. 3). Sulfate concentration showed constant values with depth in the RS (27.8 ± 0.2 mM), similar to those in seawater from the same area (28.9 mM, Paull et al., 2015), while it decreased with depth in all the MV sites and showed a concentration of ~0 mM below ~30 cmbsf at stations 17 and 18 (Fig. 3, Table S1). Phosphate and ammonium of the uppermost samples in the MV sites were on average higher than that in the RS with increasing trends shown with depth (Table 1, Table S2).

The isotopic compositions ($\delta^{18}O$ and δD) of the RS samples showed positive values, constant with depth (Fig. 4, Table 1), while these values in the MV site became more negative with depth (Fig. 4, Table S2). The data of the MV samples were displaced from the mixing line between seawater and meteoric waters (approximated by the local meteoric water line, LMWL) (Fig. 4).

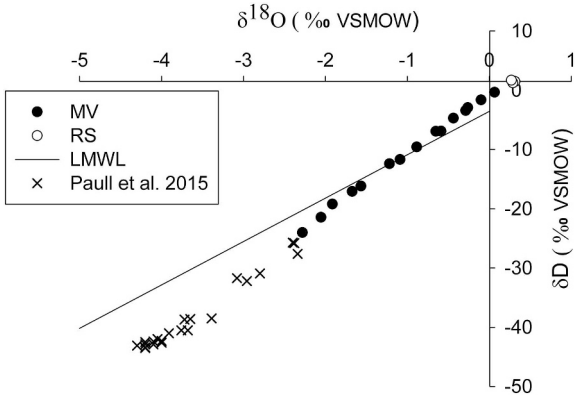


**Fig. 4.** $\delta^{18}O$ versus δD for the samples collected in the mud volcano (MV) sites (stations 15, 16, 17), in the reference site (RS), and those measured by Paull et al. (2015). The line is the projection of the local meteoric water line (LMWL) for Inuvik, Canada (http://www-naweb.iaea.org/napc/ih/IHS_resources_gnip.html).

### 3.3. Comparison of DOM between MV versus RS sites

DOC concentration in the uppermost sample in the RS was ~6 mg $L^{-1}$. A slight increase of DOC was observed at 16 cmbsf (10.5 mg $L^{-1}$), and then it showed a decreasing downward trend, reaching 5 mg $L^{-1}$ at 40 cmbsf (Fig. 5). In the MV, the DOC ranged between 14 and 49 mg $L^{-1}$ in the uppermost samples (average

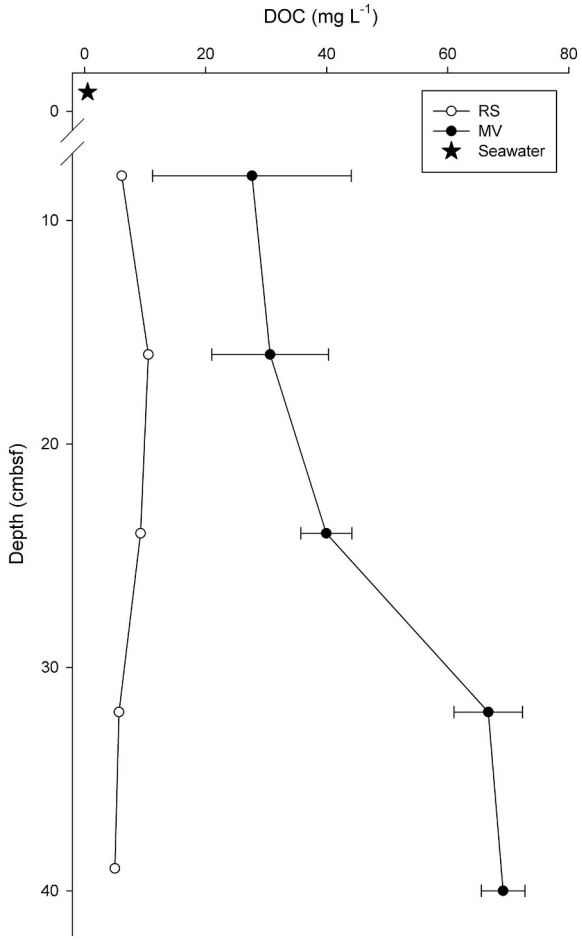


**Fig. 5.** DOC vertical distribution in the in the mud volcano sites (MV, average ± standard deviation of the four stations), in the reference site (RS) and in bottom seawater. The concentration of bottom seawater in the Canada Basin is from Griffith et al. (2012).

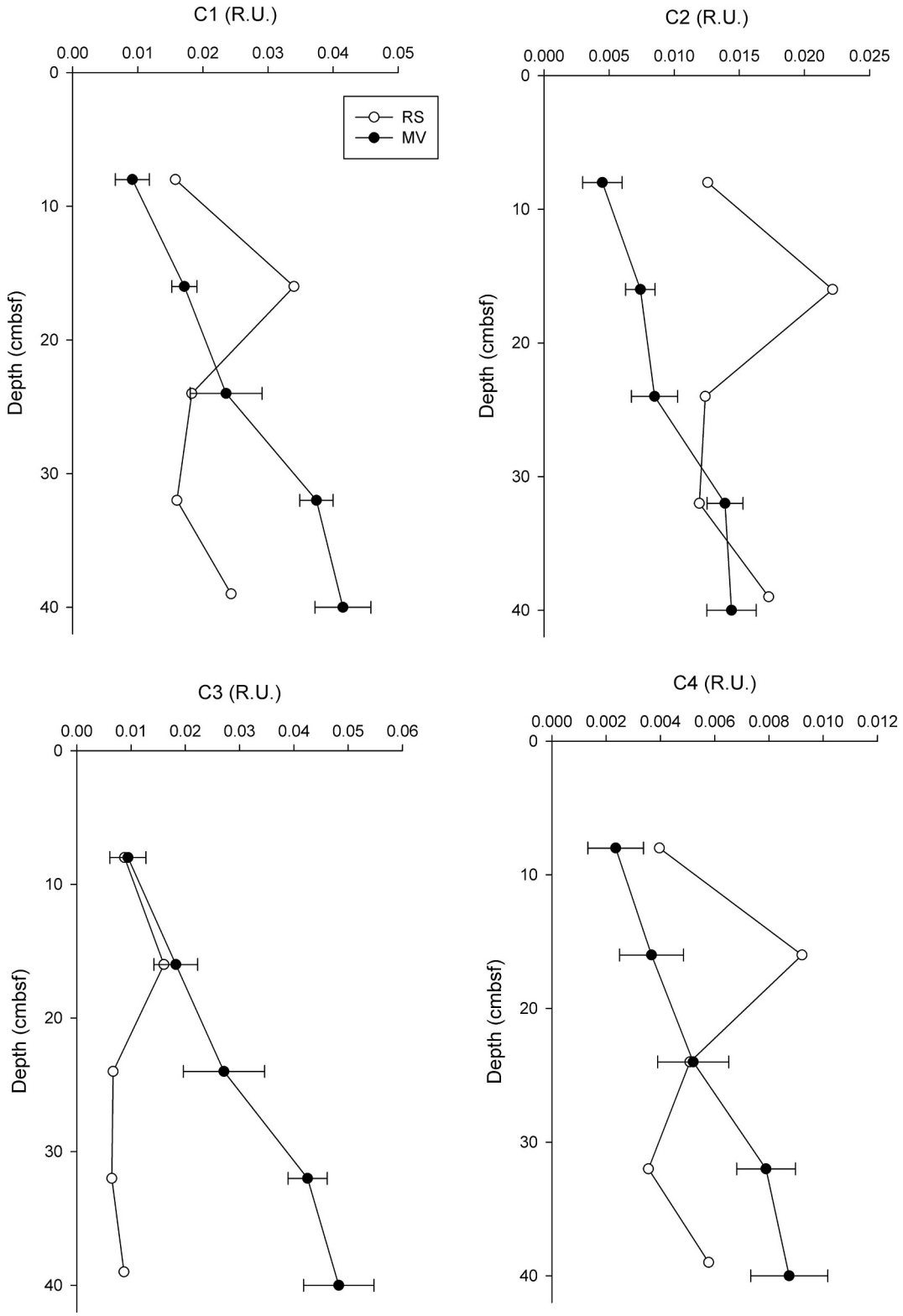


**Fig. 6.** Fluorescence components vertical distribution in the in the mud volcano sites (MV, average ± standard deviation of the four stations) and in the reference site (RS).

28 ± 16 mg $L^{-1}$) and increased up to 64–72 mg $L^{-1}$ at ~40 cmbsf (average 69 ± 4 mg $L^{-1}$). All the MV sites showed a similar downcore profile of DOC with a steep increase in the concentration below 24 cmbsf (Fig. 5, Table S2).

DOC showed good linear relationships with chloride concentrations ($R^2$ = 0.75, p < .0001, $n$ = 24), with alkalinity ($R^2$ = 0.84, p < .0001, $n$ = 24), and with sulfate concentrations ($R^2$ = 0.74, p < .0001, $n$ = 24) (Fig. S1). In the MV, DOC had also a good correlation with the freshening ratios ($R^2$ = 0.64, p < .0001, $n$ = 19).

In the MV, the downcore profiles of the four fluorescent components were similar to those of DOC, showing increasing trends with depth, although it was less pronounced for C2 (Fig. 6). The total fluorescence

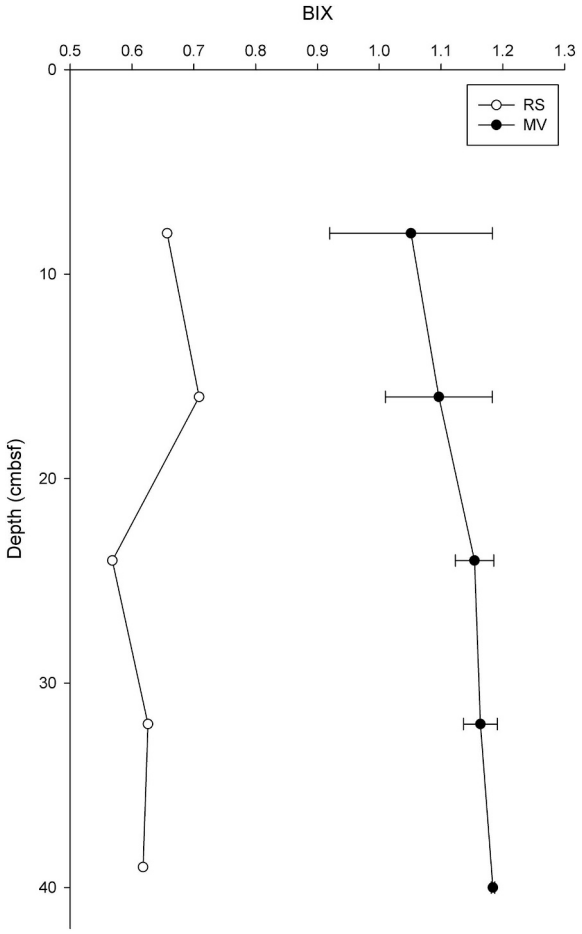


**Fig. 7.** Vertical distribution of BIX values in the mud volcano sites (MV, average ± standard deviation of the four stations) and in the reference site (RS).

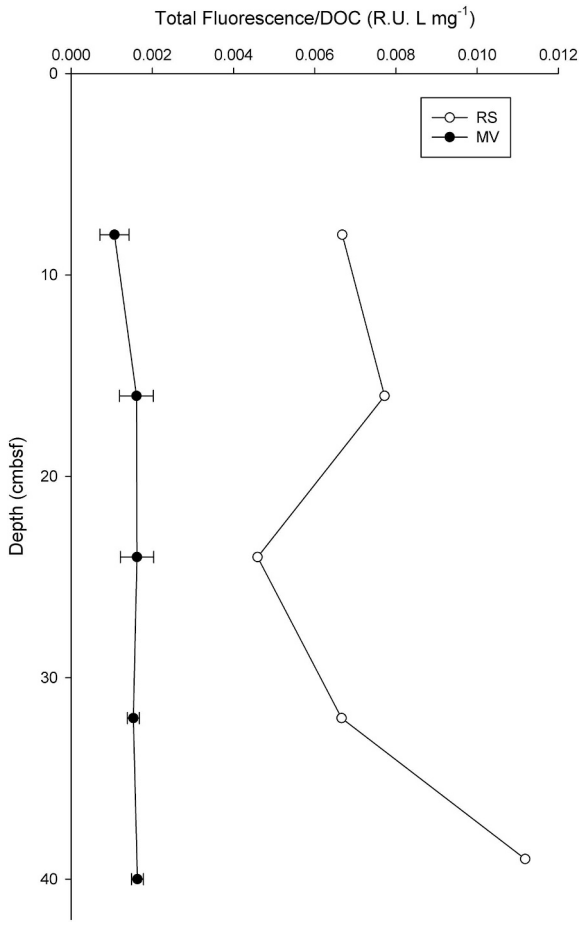


**Fig. 8.** Vertical distribution of the total fluorescence normalized by DOC concentration in the mud volcano sites (MV, average ± standard deviation of the four stations) and in the reference site (RS).

showed indeed a good linear relationship with DOC concentrations ($R^2 = 0.62$, $p < .0001$, $n = 25$). In the RS, there was no increasing or decreasing trend with depth. A relatively high fluorescence intensity was consistently observed at 16 cmbsf for all four components. Such a variation was less marked for C3. The differences in the fluorescence intensities between the MV and RS were not so pronounced as those of DOC.

The BIX was different between the MV and the RS, with the average values 1.5–2 times higher in the MV versus the RS. The variations in the index with depth were very small in both RS and MV (Fig. 7).

In order to exclude the DOC concentration effects from the fluorescence dynamics, the fluorescence intensities of the components were normalized by the corresponding DOC in the MV and RS sites. Further, since no major difference was found in the downcore profiles of the four DOC-normalized components in the MV (Fig. S2), the results for the total fluorescence (calculated as the sum of the fluorescence of the four components for each sample) are presented here. The DOC-normalized fluorescence showed an entirely different behavior from the original fluorescence data. It is noteworthy that the fluorescence in the RS is ~3 to 7 times higher than in the MV sites (Fig. 8). Despite the normalization, the vertical trend of the total fluorescence in the RS still remained unchanged. On the contrary, the DOC-normalized fluorescence intensities of the MV samples showed different dynamics with respect to the original fluorescence (Fig. 8) with much less downward variations.

## 4. Discussion

### 4.1. Origins of the four fluorescent components

The spectra of the four components validated by PARAFAC analysis were compared with those previously reported in the literature by using the OpenFluor database (Murphy et al., 2014). The comparison with the database found 26 matches with a similarity score > 0.95 (Table S2), with components originating from a wide range of environments. Moreover, the components were comparable with those from other porewater systems not present in the database (Chen et al., 2016; Luek et al., 2017; Wang et al., 2013; Yang et al., 2017) (Table S2). C1 and C2 showed excitation and emission maxima at long wavelengths, these characteristics have been usually attributed to terrestrial humic-like fluorescence (Gonçalves-Araujo et al., 2015; Osburn et al., 2016a,b; Stedmon et al., 2007; Walker et al., 2009). However, some laboratory experiments showed that these components could also be related to the activity of sulfate-reducing bacteria in anoxic sediments (Luek et al., 2017) or to the release by cyanobacteria (Bittar et al., 2015) and phytoplankton (Fukuzaki et al., 2014). C3 showed an emission maximum at lower wavelengths with respect to C1 and C2. According to the previous reports, its signal can be attributed to the so-called microbial humic-like fluorescence (Chen et al., 2016; Yamashita et al., 2010; Yang et al., 2017). C4 had excitation and emission maxima typical of protein-like fluorescence, which may be associated with the presence of tyrosine (Chen et al., 2016; Graeber et al., 2012; Yamashita et al., 2013).

### 4.2. Differences in porewaters geochemistry and DOM between the MV versus the RS

Porewaters from the MV sites clearly revealed the occurrence of fluid freshening, which can be triggered by processes such as gas hydrate dissociation, meteoric water input, and dehydration reactions (Kastner et al., 1991; Kim et al., 2013; Paull et al., 2015). When gas hydrate dissociation occurs, both δD and $\delta^{18}O$ values are enriched (e.g., Dählmann and de Lange, 2003; Hesse, 2003) with depleted $Cl^-$ concentration. The values of δD and $\delta^{18}O$ in the MV were not consistent with this reaction, thus this process was excluded as a source of freshening. The good relationship between $\delta^{18}O$ and δD of the MV samples and their displacement from the LMWL (Fig. 4) indicated that the simple mixture of seawater and meteoric water cannot fully explain the origin of these fluids. Since the geothermal gradient at this MV has a high value of ~2 °C/m (Paull et al., 2015), clay dehydration can be another potential source for the freshening. In general, clay dehydration (i.e. smectite-illite transformation) occurs between 60 and 160 °C (Freed and Peacor, 1989; Kastner et al., 1991; Kim et al., 2013; Reitz et al., 2011) and produces waters with positive $\delta^{18}O$, negative δD, and low $Cl^-$ values (Dählmann and de Lange, 2003; Kastner et al., 1991; Kim et al., 2013). However, this isotopic trend of clay dehydration is difficult to recognize in the shallow porewater when this fluid is mixed with meteoric water having depleted $\delta^{18}O$ and δD values (Kim et al., 2013; Paull et al., 2015). Hence, it can be postulated that the fluid freshening in the MV may be derived from the mixed sources (or end members) of meteoric water and clay dehydration. These results are in good agreement with those reported by Paull et al. (2015) in the same area (Fig. 4). The similarity between $\delta^{18}O$ and δD, sulfate and chloride values between this study and Paull et al. (2015) indicates that the sources of the porewater are the same.

By using the relationship between $\delta^{18}O$ and $Cl^-$ (Fig. S3) it was possible to estimate a $\delta^{18}O$ value of −5.9‰ of the freshwater component ($\delta^{18}O_{fw}$, containing both clay-derived and meteoric water) at zero $Cl^-$. The $\delta^{18}O$ of clay dehydration-derived water ($\delta^{18}O_{clay}$) was calculated according to Hensen et al. (2004) at 60 and 160 °C, temperature range reported for the clay minerals dehydration process. The $\delta^{18}O$ values obtained were 17.9 and 8.5‰ at 60 °C and 160 °C, respectively. A two-component mixing relationship was then used to estimate the contribution of the two end-members (clay and meteoric water) according to the following calculation.

$$\delta^{18}O_{clay} \cdot \%_{clay} + \delta^{18}O_{met} \cdot \%_{met} = \delta^{18}O_{fw}.$$

By using a $\delta^{18}O$ value of −22‰ for the meteoric waters ($\delta^{18}O_{met}$) reported by (Gwiazda et al., 2018), it was estimated that clay dehydration contributes ~40 to 53% (assuming the temperature of 60 °C and 160 °C, respectively) to the freshwater in the MV.

Meanwhile, the positive values of $\delta^{18}O$ and δD, the higher chlorinity, and the constant values of these parameters with depth in the RS suggest that these porewaters may be influenced by seawater only.

The freshening ratio gives an estimate of the degree of mixing between seawater and the emerging freshwater. Seawater seems to be predominant in the uppermost sample (8 cmbsf) as indicated by the freshening ratio of ~3%. Moving deeper, the influence of freshwater was more pronounced, reaching a freshening ratio of 38% at the 40 cmbsf. The good correlation between DOC and the chloride/freshening ratio suggest that the fresher waters moving upward from the deeper sediments contain a higher DOC concentration. This can give an explanation to the higher DOC concentration in the MV versus the RS and the higher DOC concentrations in the deeper MV sediments. However, the low $R^2$ of the relationship between DOC and chloride (0.75, Fig. S1) suggests that there might be other factors shaping the final DOC concentrations.

The high abundance of methane (Lee et al., 2018; Paull et al., 2015), the decrease in $SO_4^{2-}$ and the increase in alkalinity, suggest the presence of in-situ microbially-mediated processes such as particulate organic matter sulfate reduction (POCSR: $2CH_2O + SO_4^{2-} \rightarrow H_2S + 2HCO^{3-}$) and anaerobic oxidation of methane (AOM: $CH_4 + SO_4^{2-} \rightarrow HS^- + HCO^{3-} + H_2O$). These processes have been also observed in Arctic porewaters (Chen et al., 2016), although Chen et al. reported these processes occurring in the deeper sediments compared to those of the current study. Lee et al. (2018) showed the presence of a microbial community mediating AOM in the upper 2 m sediments of this MV. They also estimated that the contribution of this process to the organic carbon pool is low. The POCSR can also contribute to the DOC pool (Hong et al., 2014; Komada et al., 2016), however, the marked increase in alkalinity suggest that this process mainly produce inorganic carbon.

The increase of DOC can be also attributed to the direct release from microorganisms. The direct and/or indirect contribution of biological activity is also supported by higher BIX values in the MV versus the RS, suggesting more abundance of DOM with biological sources in the MV. The biological release of DOC has been previously reported at different seep environment in the Hydrate Ridge (Valentine et al., 2005), where enhanced heterotrophic microbial activity was observed at the seep sites compared to a reference site. These authors highlighted the important role of the advective DOC flux as a source of energy for the microbial community. The deep DOC may stimulate the microbial community, which can, in turn, release autochthonous organic materials. Moreover, a laboratory experiment demonstrated an exponential increase in DOC concentration with increasing temperature (up to ~100 °C) through abiotic processes (Lin et al., 2017).

In the RS, the increases in DOC and FDOM at 16 cmbsf corresponded to the increases of Fe and Mn (Table S2). This observation suggests that this slight increase might be attributed to a reductive dissolution of Fe−/ Mn-oxides, which can release the absorbed materials into the porewaters (Chen and Hur, 2015; Deflandre et al., 2002; O'Loughlin and Chin, 2004; Sierra et al., 2001).

The fluorescence results indicate that the FDOM properties in the MV sites are similar to those previously reported for porewaters in other areas (Chen et al., 2016; Wang et al., 2013; Yang et al., 2017), suggesting that the peculiarity of this environment might not affect the main fluorescent composition of porewater DOM. The similar vertical distribution of the four fluorescent components further suggests that within the investigated depth there was not a change in FDOM composition. Only C3 showed slightly different dynamics with respect to the other three components, with the higher fluorescence intensity in the MV versus the RS sites, which supports a potentially higher biological activity in the MV.

It is noteworthy that the DOC-normalized fluorescence in the MV sites was considerably lower than that of the RS (3 to 7 times). This suggests that there might be some factors quenching the fluorescence in the MV porewaters. Factors such as pH, the presence of metals (e.g. Fe) and oxygenation during and/or after sampling can affect DOM fluorescence. Considering the narrow range of variation of the pH both in depth and between the MV and the RS (Table S2) we can exclude a significant effect of pH on FDOM (Spencer and Coble, 2014). DOM-metal binding can also quench the fluorescence. However, the concentration of the measured metals (e.g. Fe) was higher in the RS site than in the MV sites (Table S2), thus we should have a higher quenching in the RS. We, therefore, excluded a significant quenching effect of metals (i.e. Fe). Regarding a possible effect of the oxygenation of the samples after extraction, several precautions were taken to keep the oxygenation at a minimum (vacuum extraction, immediate filtration, and freezing). Moreover, taking into account the results of Luek et al. (2017), we assumed that, even if there is a quenching effect due to oxygenation, this would be minimum compared to the difference between the MV and RS sites. A lower fluorescence might be attributed to an intrinsic lower fluorescence of the molecules released by in situ biological activity. This hypothesis can, however, be excluded considering the results of Luek et al. (2017), which showed an increase in fluorescence in correspondence with sulfate reduction and sulfate-reducing bacteria activity in an incubation experiment with anoxic

sediments. Finally, the lower fluorescence of the MV samples may result from the thermal quenching of the fluorophores at high temperatures. Previous studies showed that a higher thermal maturity increases the concentrations of the fluorophores leading to a deterioration of fluorescence emission by increasing quenching phenomena (Pradier et al., 1991 and references therein). According to Pradier et al. (1991), organic matter fluorescence starts to decrease when its thermal maturity enters the oil window (temperature > 60 °C). The porewaters in the MV sites are indeed affected by higher temperatures with respect to the RS as demonstrated by Paull et al. (2015), which showed that geothermal gradient was significantly higher in the MV sites (~2 °C/m) than in the RS (~0.08 °C/m). Clay dehydration, which is one of the end members of these mixed fluids, can also occur at the same temperature (≥ 60 °C). Baker (2005) also pointed out the importance of the thermal quenching phenomenon and suggested that the difference in the quenching can be attributed to the different sources and chemical nature of the specific fluorescent compounds. The constant values with depth of the DOC-normalized total fluorescence in the MV indicate invariant DOM composition within the depths investigated.

From the results of DOC-normalized fluorescence, we can hypothesize that most of the DOM in the surface sediments of the MV is coming from the deeper sediments and has undergone thermogenic processes. This is in agreement with the identification of thermogenic compounds in deep-sea water DOM (Dittmar and Koch, 2006). Shallow processes seem not to affect significantly FDOM composition. However, more specific analysis (e.g. C isotopes, FT-ICR-MS) should be carried out in order to confirm this hypothesis.

## 5. Summary and conclusions

This study reported, for the first time, direct measurements of the porewater DOM properties in the 420 MV in the Canadian Beaufort Sea. The results highlighted a significant freshening of the porewaters within the MV, confirming previous findings on this site. The emerging fluids are characterized by a DOC concentration up to 14 times higher than the RS, signifying the high contribution that this area can have to deep seawater DOC. The very low DOC-normalized fluorescence in the MV sites was attributed to the thermogenic processes affecting these fluids in the deeper sediments. This parameter (DOC-normalized fluorescence) might, therefore, be a useful proxy to identify the deep fluids DOM undergone thermogenic processes. The similarity of the FDOM components, identified using PARAFAC analysis, with porewater in other environments suggest that this peculiar environment might not affect the characteristics of DOM fluorescence. The results of the intrinsic fluorescence suggested that the main factor controlling the DOM properties in this environment is the input from the deep fluids and that the in-situ processes do not significantly affect FDOM composition. However, it must be taken into account that what we observed is the result of several processes occurring within the MV that cannot be quantified and are difficult to discriminate with the available measurements. More specific analysis (e.g. C isotopes, FT-ICR-MS) and deeper samples are therefore needed to confirm our hypothesis.

In general, the findings of this study highlighted the importance of MV in the deep waters carbon cycle, especially because the extrusion of fluids is a continuous process in time. In order to improve the global estimates of DOC from sediments and its relevance in the deep waters, further studies are needed to estimate the flux of DOC from these areas, by direct measurements, and to gain information on the reactivity of the released DOM.

## Acknowledgments

This work was supported by a National Research Foundation of Korea (NRF) grant funded by the Korean government (MSIP) (No. 2017R1A4A1015393) and by the Korea Polar Research Institute Grants PM18050 (KIMST Grant 20160247).

## Appendix A. Supplementary data

Supplementary data to this article can be found online at https://doi.org/10.1016/j.marchem.2019.03.009.

## References

Baker, A., 2005. Thermal fluorescence quenching properties of dissolved organic matter. Water Res. 39, 4405–4412. https://doi.org/10.1016/j.watres.2005.08.023.
Bittar, T.B., Vieira, A.A.H., Stubbins, A., Mopper, K., 2015. Competition between photochemical and biological degradation of dissolved organic matter from the cyanobacteria *Microcystis aeruginosa*. Limnol. Oceanogr. 60, 1172–1194. https://doi.org/10.1002/lno.10090.
Burdige, D.J., 2007. Preservation of organic matter in marine sediments: controls, mechanisms, and an imbalance in sediment organic carbon budgets? Chem. Rev. 107, 467–485. https://doi.org/10.1021/cr050347q.
Burdige, D.J., Komada, T., 2015. Sediment pore waters. In: Biogeochemistry of Marine Dissolved Organic Matter, 2nd ed. pp. 535–577. https://doi.org/10.1016/B978-0-12-405940-5.00012-1.
Chen, M., Hur, J., 2015. Pre-treatments, characteristics, and biogeochemical dynamics of dissolved organic matter in sediments: a review. Water Res. 79, 10–25.
Chen, M., Kim, J.-H., Nam, S.-I., Niessen, F., Hong, W.-L., Kang, M.-H., Hur, J., 2016. Production of fluorescent dissolved organic matter in Arctic Ocean sediments. Sci. Rep. 6, 39213. https://doi.org/10.1038/srep39213.
Cita, M.B., Camerlenghi, A., Erba, E., McCoy, F.W., Castradori, D., Cazzani, A., Guasti, G., Giambastiani, G., Lucchi, R., Nolli, V., Pezzi, G., Redaelli, M., Rizzi, E., Torricelli, S., Violanti, D., 1989. Discovery of mud diapirism on the Mediterranean ridge; a preliminary report. Ital. J. Geosci. 108, 537–543.
Clark, I., Fritz, P., 1997. Environmental Isotopes in Hydrology. Science.
Connolly, J.A.D., Podladchikov, Y.Y., 2016. An analytical solution for solitary porosity waves: dynamic permeability and fluidization of nonlinear viscous and viscoplastic rock. Geofluids 15, 269–292. https://doi.org/10.1002/9781119166573.ch23.
Dählmann, A., de Lange, G.J., 2003. Fluid-sediment interactions at eastern Mediterranean mud volcanoes: a stable isotope study from ODP leg 160. Earth Planet. Sci. Lett. 212, 377–391. https://doi.org/10.1016/S0012-821X(03)00227-9.
Dang, D.H., Lenoble, V., Durrieu, G., Mullot, J.-U., Mounier, S., Garnier, C., 2014. Sedimentary dynamics of coastal organic matter: an assessment of the porewater size/reactivity model by spectroscopic techniques. Estuar. Coast. Shelf Sci. 151, 100–111. https://doi.org/10.1016/J.ECSS.2014.10.002.
Deflandre, B., Mucci, A., Gagné, J.-P., Guignard, C., Sundby, B.jør., 2002. Early diagenetic processes in coastal marine sediments disturbed by a catastrophic sedimentation event. Geochim. Cosmochim. Acta 66, 2547–2558. https://doi.org/10.1016/S0016-7037(02)00861-X.
Dittmar, T., Koch, B.P., 2006. Thermogenic organic matter dissolved in the abyssal ocean. Mar. Chem. 102, 208–217. https://doi.org/10.1016/j.marchem.2006.04.003.
Frederick, J.M., Buffett, B.A., 2014. Taliks in relict submarine permafrost and methane hydrate deposits: pathways for gas escape under present and future conditions. J. Geophys. Res. Earth Surf. 119, 106–122. https://doi.org/10.1002/2013JF002987.
Freed, R.L., Peacor, D.R., 1989. Geopressured shale and sealing effect of smectite to illite transition. Am. Assoc. Pet. Geol. Bull. 73, 1223–1232. https://doi.org/10.1306/44B4AA0A-170A-11D7-8645000102C1865D.
Fukuzaki, K., Imai, I., Fukushima, K., Ishii, K.-I.I., Sawayama, S., Yoshioka, T., 2014. Fluorescent characteristics of dissolved organic matter produced by bloom-forming coastal phytoplankton. J. Plankton Res. 36, 685–694. https://doi.org/10.1093/plankt/fbu015.
Gat, J.R., 1996. Oxygen and hydrogen isotopes in the hydrologic cycle. Annu. Rev. Earth Planet. Sci. 24, 225–262. https://doi.org/10.1159/000088336.
Gieskes, J.M., Gamo, T., Brumsack, H., 1991. Chemical methods for interstitial water analysis aboard JOIDES resolution. Ocean Drill. Progr. Texas A&M Univ. Tech. Note 15, 1–60. https://doi.org/10.2973/odp.tn.15.1991.
Gonçalves-Araujo, R., Stedmon, C.A., Heim, B., Dubinenkov, I., Kraberg, A., Moiseev, D., Bracher, A., 2015. From fresh to marine waters: characterization and fate of dissolved organic matter in the Lena River Delta region, Siberia. Front. Mar. Sci. 2, 108. https://doi.org/10.3389/fmars.2015.00108.
Graeber, D., Gelbrecht, J., Pusch, M.T., Anlanger, C., von Schiller, D., 2012. Agriculture has changed the amount and composition of dissolved organic matter in central European headwater streams. Sci. Total Environ. 438, 435–446. https://doi.org/10.1016/j.scitotenv.2012.08.087.
Grantz, A., Hart, P.E., 2012. Petroleum prospectivity of the Canada Basin, Arctic Ocean. Mar. Pet. Geol. 30 (1), 126–143. https://doi.org/10.1016/j.marpetgeo.2011.11.001.
Griffith, D.R., McNichol, A.P., Xu, L., McLaughlin, F.A., Macdonald, R.W., Brown, K.A., Eglinton, T.I., 2012. Carbon dynamics in the western Arctic Ocean: insights from full-depth carbon isotope profiles of DIC, DOC, and POC. Biogeosciences 9, 1217–1224. https://doi.org/10.5194/bg-9-1217-2012.
Gwiazda, R., Paull, C.K., Dallimore, S.R., Melling, H., Jin, Y.K., Hong, J.K., Riedel, M., Lundsten, E., Anderson, K., Conway, K., 2018. Freshwater seepage into sediments of the shelf, shelf edge, and continental slope of the Canadian Beaufort Sea. Geochem. Geophys. Geosyst. 19 (9), 3039–3055. https://doi.org/10.1029/2018GC007623.
Haese, R.R., Hensen, C., de Lange, G.J., 2006. Pore water geochemistry of eastern Mediterranean mud volcanoes: implications for fluid transport and fluid origin. Mar. Geol. 225, 191–208. https://doi.org/10.1016/J.MARGEO.2005.09.001.
Henrichs, S.M., 1992. Early diagenesis of organic matter in marine sediments: progress and perplexity. Mar. Chem. 39, 119–149. https://doi.org/10.1016/0304-4203(92)90098-U.
Hensen, C., Wallmann, K., Schmidt, M., Ranero, C.R., Suess, E., 2004. Fluid expulsion related to mud extrusion off Costa Rica – a window to the subducting slab. Geology. 32 (3), 201–204. https://doi.org/10.1130/G20119.1.
Hesse, R., 2003. Pore water anomalies of submarine gas-hydrate zones as tool to assess

hydrate abundance and distribution in the subsurface what have we learned in the past decade? Earth-Sci. Rev. 61 (1-2), 149–179. https://doi.org/10.1016/S0012-8252(02)00117-4.
Hong, W.-L., Torres, M.E., Kim, J.-H., Choi, J., Bahk, J.-J., 2014. Towards quantifying the reaction network around the sulfate–methane-transition-zone in the Ulleung Basin, East Sea, with a kinetic modeling approach. Geochim. Cosmochim. Acta 140, 127–141. https://doi.org/10.1016/J.GCA.2014.05.032.
Huguet, a., Vacher, L., Relexans, S., Saubusse, S., Froidefond, J.M., Parlanti, E., 2009. Properties of fluorescent dissolved organic matter in the Gironde estuary. Org. Geochem. 40, 706–719. https://doi.org/10.1016/j.orggeochem.2009.03.002.
Jin, Y.K., Shipboard Scientific Party, 2018. ARA08C Cruise Report: 2017 Korea-Canada-USA Beaufort Sea Research Program. Korea Polar Research Institute.
Jung, Y.-Y., Koh, D.-C., Lee, J., Ko, K.-S., 2013. Applications of isotope ratio infrared spectroscopy (IRIS) to analysis of stable isotopic compositions of liquid water. Econ. Environ. Geol. 46, 495–508. https://doi.org/10.9719/EEG.2013.46.6.495.
Kastner, M., Elderfield, H., Martin, J.B., 1991. Fluids in convergent margins: what do we know about their composition, origin, role in diagenesis and importance for oceanic chemical fluxes? Philos. Trans. R. Soc. Londn. Ser. A Phys. Eng. Sci. 335, 243–259. https://doi.org/10.1098/rsta.1991.0045.
Kendall, C., Caldwell, E.A., 1998. Isotope Tracers in catchment hydrology, in: Fundamentals of Isotope Geochemistry. doi:https://doi.org/10.1016/B978-0-444-81546-0.50010-0.
Kim, J.-H., Torres, M.E., Hong, W.-L., Choi, J., Bahk, J.-J., Kim, S.-H., 2013. Pore fluid chemistry from the second gas hydrate drilling expedition in the Ulleung Basin (UBGH2): source, mechanisms and consequences of fluid freshening in the central part of the Ulleung Basin, East Sea. Mar. Pet. Geol. 47, 99–112. https://doi.org/10.1016/J.MARPETGEO.2012.12.011.
Komada, T., Burdige, D.J., Crispo, S.M., Druffel, E.R.M., Griffin, S., Johnson, L., Le, D., 2013. Dissolved organic carbon dynamics in anaerobic sediments of the Santa Monica Basin. Geochim. Cosmochim. Acta 110, 253–273. https://doi.org/10.1016/J.GCA.2013.02.017.
Komada, T., Burdige, D.J., Li, H.-L., Magen, C., Chanton, J.P., Cada, A.K., 2016. Organic matter cycling across the sulfate-methane transition zone of the Santa Barbara Basin, California borderland. Geochim. Cosmochim. Acta 176, 259–278. https://doi.org/10.1016/J.GCA.2015.12.022.
Kopf, A.J., 2002. Significance of mud volcanism. Rev. Geophys. 40. https://doi.org/10.1029/2000RG000093.
Korak, J.A., Dotson, A.D., Summers, R.S., Rosario-Ortiz, F.L., 2014. Critical analysis of commonly used fluorescence metrics to characterize dissolved organic matter. Water Res. 49, 327–338. https://doi.org/10.1016/j.watres.2013.11.025.
Lee, D.-H., Kim, J.-H., Lee, Y.M., Stadnitskaia, A., Jin, Y.K., Niemann, H., Kim, Y.-G., Shin, K.-H., 2018. Biogeochemical evidence of anaerobic methane oxidation on active submarine mud volcanoes on the continental slope of the Canadian Beaufort Sea. Biogeosciences 15, 7419–7433. https://doi.org/10.5194/bg-15-7419-2018.
Li, N., Huang, H., Chen, D., 2014. Fluid sources and chemical processes inferred from geochemistry of pore fluids and sediments of mud volcanoes in the southern margin of the Junggar Basin, Xinjiang, northwestern China. Appl. Geochem. 46, 1–9. https://doi.org/10.1016/J.APGEOCHEM.2014.04.007.
Lin, Y.S., Koch, B.P., Feseker, T., Ziervogel, K., Goldhammer, T., Schmidt, F., Witt, M., Kellermann, M.Y., Zabel, M., Teske, A., Hinrichs, K.U., 2017. Near-surface heating of young rift sediment causes mass production and discharge of reactive dissolved organic matter. Sci. Rep. 7, 44864. https://doi.org/10.1038/srep44864.
Loher, M., Pape, T., Marcon, Y., Römer, M., Wintersteller, P., Praeg, D., Torres, M., Sahling, H., Bohrmann, G., 2018. Mud extrusion and ring-fault gas seepage – upward branching fluid discharge at a deep-sea mud volcano. Sci. Rep. 8, 6275. https://doi.org/10.1038/s41598-018-24689-1.
Lösekann, T., Robador, A., Niemann, H., Knittel, K., Boetius, A., Dubilier, N., 2008. Endosymbioses between bacteria and deep-sea siboglinid tubeworms from an Arctic cold seep (Haakon Mosby mud volcano, Barents Sea). Environ. Microbiol. 10, 3237–3254. https://doi.org/10.1111/j.1462-2920.2008.01712.x.
Luek, J.L., Thompson, K.E., Larsen, R.K., Heyes, A., Gonsior, M., 2017. Sulfate reduction in sediments produces high levels of chromophoric dissolved organic matter. Sci. Rep. 7, 8829. https://doi.org/10.1038/s41598-017-09223-z.
Mazzini, A., Etiope, G., 2017. Mud volcanism: an updated review. Earth-Sci. Rev. 168, 81–112. https://doi.org/10.1016/j.earscirev.2017.03.001.
Milkov, A.V., 2000. Worldwide distribution of submarine mud volcanoes and associated gas hydrates. Mar. Geol. 167, 29–42. https://doi.org/10.1016/S0025-3227(00)00022-0.
Milkov, A.V., Vogt, P.R., Crane, K., Lein, A.Y., Sassen, R., Cherkashev, G.A., 2004. Geological, geochemical, and microbial processes at the hydrate-bearing Håkon Mosby mud volcano: a review. Chem. Geol. 205, 347–366. https://doi.org/10.1016/j.chemgeo.2003.12.030.
Minami, H., Hachikubo, A., Yamashita, S., Sakagami, H., Kasashima, R., Konishi, M., Shoji, H., Takahashi, N., Pogodaeva, T., Krylov, A., Khabuev, A., Kazakov, A., De Batist, M., Naudts, L., Chensky, A., Gubin, N., Khlystov, O., 2018. Hydrogen and oxygen isotopic anomalies in pore waters suggesting clay mineral dehydration at gas hydrate-bearing Kedr mud volcano, southern Lake Baikal, Russia. Geo-Mar. Lett. 38, 403–415. https://doi.org/10.1007/s00367-018-0542-x.
Murphy, K.R., Butler, K.D., Spencer, R.G.M., Stedmon, C.A., Boehme, J.R., Aiken, G.R., 2010. Measurement of dissolved organic matter fluorescence in aquatic environments: an Interlaboratory comparison. Environ. Sci. Technol. 44, 9405–9412. https://doi.org/10.1021/es102362t.
Murphy, K.R., Stedmon, C.A., Graeber, D., Bro, R., 2013. Fluorescence spectroscopy and multi-way techniques. PARAFAC. Anal. Methods 5, 6557. https://doi.org/10.1039/c3ay41160e.
Murphy, K.R., Stedmon, C.A., Wenig, P., Bro, R., 2014. OpenFluor- an online spectral library of auto-fluorescence by organic compounds in the environment. Anal. Methods 6, 658–661. https://doi.org/10.1039/C3AY41935E.
O'Loughlin, E.J., Chin, Y.-P., 2004. Quantification and characterization of dissolved organic carbon and iron in sedimentary porewater from Green Bay, WI, USA. Biogeochemistry 71, 371–386. https://doi.org/10.1007/s10533-004-0373-x.
Osburn, C.L., Boyd, T.J., Montgomery, M.T., Bianchi, T.S., Coffin, R.B., Paerl, H.W., 2016a. Optical proxies for terrestrial dissolved organic matter in estuaries and coastal waters. Front. Mar. Sci. 2, 127. https://doi.org/10.3389/fmars.2015.00127.
Osburn, C.L., Handsel, L.T., Peierls, B.L., Paerl, H.W., 2016b. Predicting sources of dissolved organic nitrogen to an estuary from an agro-urban coastal watershed. Environ. Sci. Technol. 50, 8473–8484. https://doi.org/10.1021/acs.est.6b00053.
Otero, M., Mendonça, A., Válega, M., Santos, E.B.H., Pereira, E., Esteves, V.I., Duarte, A., 2007. Fluorescence and DOC contents of estuarine pore waters from colonized and non-colonized sediments: effects of sampling preservation. Chemosphere 67, 211–220. https://doi.org/10.1016/J.CHEMOSPHERE.2006.10.044.
Paull, C.K., Dallimore, S., Hughes-Clarke, J., Blasco, S., Lundsten, E., Ussler, W.I., Graves, D., Sherman, A., Conway, K., Melling, H., Vagle, S., Collett, T., 2011. Tracking the decomposition of permafrost and gas hydrate under the shelf and slope of the Beaufort Sea. In: Proceedings of the 7th International Conference on Gas Hydrate.
Paull, C.K., Dallimore, S.R., Caress, D.W., Gwiazda, R., Melling, H., Riedel, M., Jin, Y.K., Hong, J.K., Kim, Y.-G., Graves, D., Sherman, A., Lundsten, E., Anderson, K., Lundsten, L., Villinger, H., Kopf, A., Johnson, S.B., Hughes Clarke, J., Blasco, S., Conway, K., Neelands, P., Thomas, H., Côté, M., 2015. Active mud volcanoes on the continental slope of the Canadian Beaufort Sea. Geochem. Geophys. Geosyst. 16, 3160–3181. https://doi.org/10.1002/2015GC005928.
Pohlman, J., Bauer, J.E., Waite, W.F., Osburn, C.L., Ross Chapman, N., 2010. Methane hydrate-bearing seeps as a source of aged dissolved organic carbon to the oceans. Nat. Geosci. 4, 37–41. https://doi.org/10.1038/NGEO1016.
Pradier, B., Bertrand, P., Martinez, L., Laggoun-Defarge, F., 1991. Fluorescence of organic matter and thermal maturity assessment. Org. Geochem. 17, 511–524. https://doi.org/10.1016/0146-6380(91)90115-Z.
Qualls, R.G., Richardson, C.J., 2003. Factors controlling concentration, export, and decomposition of dissolved organic nutrients in the Everglades of Florida. Biogeochemistry 62, 197–229. https://doi.org/10.1023/A:1021150503664.
Raymond, P.A., Spencer, R.G.M., 2015. Riverine DOM. In: Biogeochemistry of marine dissolved organic matter, 2nd ed. pp. 509–533. https://doi.org/10.1016/B978-0-12-405940-5.00011-X.
Reitz, A., Pape, T., Haeckel, M., Schmidt, M., Berner, U., Scholz, F., Liebetrau, V., Aloisi, G., Weise, S.M., Wallmann, K., 2011. Sources of fluids and gases expelled at cold seeps offshore Georgia, eastern Black Sea. Geochim. Cosmochim. Acta 75, 3250–3268. https://doi.org/10.1016/J.GCA.2011.03.018.
Schulz, H.D., Dahmke, A., Schinzel, U., Wallmann, K., Zabel, M., 1994. Early diagenetic processes, fluxes, and reaction rates in sediments of the South Atlantic. Geochim. Cosmochim. Acta 58, 2041–2060. https://doi.org/10.1016/0016-7037(94)90284-4.
Sierra, M.M., Donard, O.F., Etcheber, H., Soriano-Sierra, E., Ewald, M., 2001. Fluorescence and DOC contents of pore waters from coastal and deep-sea sediments in the Gulf of Biscay. Org. Geochem. 32, 1319–1328. https://doi.org/10.1016/S0146-6380(01)00100-0.
Spencer, R.G.M., Coble, P.G., 2014. Sampling design for organic matter fluorescence analysis. In: Aquatic Organic Matter Fluorescence, pp. 125–146.
Stedmon, C.A., Markager, S., Tranvik, L., Kronberg, L., Slätis, T., Martinsen, W., 2007. Photochemical production of ammonium and transformation of dissolved organic matter in the Baltic Sea. Mar. Chem. 104, 227–240. https://doi.org/10.1016/J.MARCHEM.2006.11.005.
Taylor, A.E., Dallimore, S.R., Hill, P.R., Issler, D.R., Blasco, S., Wright, F., 2013. Numerical model of the geothermal regime on the Beaufort shelf, arctic Canada since the last interglacial. J. Geophys. Res. Earth Surf. 118, 2365–2379. https://doi.org/10.1002/2013JF002859.
Valentine, D.L., Kastner, M., Wardlaw, G.D., Wang, X., Purdy, A., Bartlett, D.H., 2005. Biogeochemical investigations of marine methane seeps, hydrate ridge, Oregon. J. Geophys. Res. Biogeosci. 110. https://doi.org/10.1029/2005JG000025.
Walker, S.A., Amon, R.M.W., Stedmon, C., Duan, S., Louchouarn, P., 2009. The use of PARAFAC modeling to trace terrestrial dissolved organic matter and fingerprint water masses in coastal Canadian Arctic surface waters. J. Geophys. Res. Biogeosci. 114. https://doi.org/10.1029/2009JG000990.
Wang, Y., Zhang, D., Shen, Z., Feng, C., Chen, J., 2013. Revealing sources and distribution changes of dissolved organic matter (DOM) in pore water of sediment from the Yangtze estuary. PLoS One 8, e76633. https://doi.org/10.1371/journal.pone.0076633.
West, A.G., February, E.C., Bowen, G.J., 2014. Spatial analysis of hydrogen and oxygen stable isotopes ("isoscapes") in ground water and tap water across South Africa. J. Geochem. Explor. 145, 213–222. https://doi.org/10.1016/J.GEXPLO.2014.06.009.
Yamashita, Y., Scinto, L.J., Maie, N., Jaffé, R., 2010. Dissolved organic matter characteristics across a subtropical Wetland's landscape: application of optical properties in the assessment of environmental dynamics. Ecosystems 13, 1006–1019. https://doi.org/10.1007/s10021-010-9370-1.
Yamashita, Y., Boyer, J.N., Jaffé, R., 2013. Evaluating the distribution of terrestrial dissolved organic matter in a complex coastal ecosystem using fluorescence spectroscopy. Cont. Shelf Res. 66, 136–144. https://doi.org/10.1016/j.csr.2013.06.010.
Yang, L., Zhuang, W.-E., Chen, C.-T.A., Wang, B.-J., Kuo, F.-W., 2017. Unveiling the transformation and bioavailability of dissolved organic matter in contrasting hydrothermal vents using fluorescence EEM-PARAFAC. Water Res. 111, 195–203. https://doi.org/10.1016/J.WATRES.2017.01.001.
Yarushina, V.M., Podladchikov, Y.Y., Connolly, J.A.D., 2015. (De)compaction of porous viscoelastoplastic media: solitary porosity waves. J. Geophys. Res. Solid Earth 120, 4843–4862. https://doi.org/10.1002/2014JB011260.